28 August 1981, Volume 213, Number 4511 SCIENCE

Climate Impact of Increasing Atmospheric Carbon Dioxide

J. Hansen, D. Johnson, A. Lacis, S. Lebedeff
P. Lee, D. Rind, G. Russell

Summary. The global temperature rose by 0.2°C between the middle 1960's and 1980, yielding a warming of 0.4°C in the past century. This temperature increase is consistent with the calculated greenhouse effect due to measured increases of atmospheric carbon dioxide. Variations of volcanic aerosols and possibly solar luminosity appear to be primary causes of observed fluctuations about the mean trend of increasing temperature. It is shown that the anthropogenic carbon dioxide warming should emerge from the noise level of natural climate variability by the end of the century, and there is a high probability of warming in the 1980's. Potential effects on climate in the 21st century include the creation of drought-prone regions in North America and central Asia as part of a shifting of climatic zones, erosion of the West Antarctic ice sheet with a consequent worldwide rise in sea level, and opening of the fabled Northwest Passage.

Atmospheric CO_2 increased from 280 to 300 parts per million in 1880 to 335 to 340 ppm in 1980 (*1, 2*), mainly due to burning of fossil fuels. Deforestation and changes in biosphere growth may also have contributed, but their net effect is probably limited in magnitude (*2, 3*). The CO_2 abundance is expected to reach 600 ppm in the next century, even if growth of fossil fuel use is slow (*4*).

Carbon dioxide absorbs in the atmospheric "window" from 7 to 14 micrometers which transmits thermal radiation emitted by the earth's surface and lower atmosphere. Increased atmospheric CO_2 tends to close this window and cause outgoing radiation to emerge from higher, colder levels, thus warming the surface and lower atmosphere by the so-called greenhouse mechanism (*5*). The most sophisticated models suggest a mean warming of 2° to 3.5°C for doubling of the CO_2 concentration from 300 to 600 ppm (*6–8*).

The major difficulty in accepting this theory has been the absence of observed warming coincident with the historic CO_2 increase. In fact, the temperature in the Northern Hemisphere decreased by about 0.5°C between 1940 and 1970 (*9*), a time of rapid CO_2 buildup. In addition, recent claims that climate models overestimate the impact of radiative perturbations by an order of magnitude (*10, 11*) have raised the issue of whether the greenhouse effect is well understood.

We first describe the greenhouse mechanism and use a simple model to compare potential radiative perturbations of climate. We construct the trend of observed global temperature for the past century and compare this with global climate model computations, providing a check on the ability of the model to simulate known climate change. Finally, we compute the CO_2 warming expected in the coming century and discuss its potential implications.

Greenhouse Effect

The effective radiating temperature of the earth, T_e, is determined by the need for infrared emission from the planet to balance absorbed solar radiation:

$$\pi R^2(1 - A)S_0 = 4\pi R^2\sigma T_e \quad (1)$$

or

$$T_e = [S_0(1 - A)/4\sigma]^{1/4} \quad (2)$$

where R is the radius of the earth, A the albedo of the earth, S_0 the flux of solar radiation, and σ the Stefan-Boltzmann constant. For $A \sim 0.3$ and $S_0 = 1367$ watts per square meter, this yields $T_e \sim 255$ K.

The mean surface temperature is $T_s \sim 288$ K. The excess, $T_s - T_e$, is the greenhouse effect of gases and clouds, which cause the mean radiating level to be above the surface. An estimate of the greenhouse warming is

$$T_s \sim T_e + \Gamma H \quad (3)$$

where H is the flux-weighted mean altitude of the emission to space and Γ is the mean temperature gradient (lapse rate) between the surface and H. The earth's troposphere is sufficiently opaque in the infrared that the purely radiative vertical temperature gradient is convectively unstable, giving rise to atmospheric motions that contribute to vertical transport of heat and result in $\Gamma \sim 5°$ to 6°C per kilometer. The mean lapse rate is less than the dry adiabatic value because of latent heat release by condensation as moist air rises and cools and because the atmospheric motions that transport heat vertically include large-scale atmospheric dynamics as well as local convection. The value of H is ~5 km at midlatitudes (where $\Gamma \sim 6.5°C\ km^{-1}$) and ~6 km in the global mean ($\Gamma \sim 5.5°C\ km^{-1}$).

The surface temperature resulting from the greenhouse effect is analogous to the depth of water in a leaky bucket with constant inflow rate. If the holes in the bucket are reduced slightly in size, the water depth and water pressure will

The authors are atmospheric physicists at the NASA Institute for Space Studies, Goddard Space Flight Center, New York 10025. D. Johnson contributed to the carbon dioxide research as a participant in the Summer Institute on Planets and Climate at the Goddard Institute for Space Studies and Columbia University.

0036-8075/81/0828-0957$01.00/0

increase until the flow rate out of the holes again equals the inflow rate. Analogously, if the atmospheric infrared opacity increases, the temperature of the surface and atmosphere will increase until the emission of radiation from the planet again equals the absorbed solar energy.

The greenhouse theory can be tested by examination of several planets, which provide an ensemble of experiments over a wide range of conditions. The atmospheric composition of Mars, Earth, and Venus lead to mean radiating levels of about 1, 6, and 70 km, and lapse rates of $\Gamma \sim 5°$, 5.5°, and 7°C km^{-1}, respectively. Observed surface temperatures of these planets confirm the existence and order of magnitude of the predicted greenhouse effect (Eq. 3). Data now being collected by spacecraft at Venus and Mars (*12*) will permit more precise analyses of radiative and dynamical mechanisms that affect greenhouse warming.

One-Dimensional Model

A one-dimensional radiative-convective (1-D RC) model (*5, 13*), which computes temperature as a function of altitude, can simulate planetary temperatures more realistically than the zero-dimensional model of Eq. 1. The sensitivity of surface temperature in 1-D RC models to changes in CO_2 is similar to the sensitivity of mean surface temperature in global three-dimensional models (*6–8*). This agreement does not validate the models; it only suggests that one-dimensional models can simulate the effect of certain basic mechanisms and feedbacks. But the agreement does permit useful studies of global mean temperature change with a simple one-dimensional model.

The 1-D RC model uses a time-marching procedure to compute the vertical temperature profile from the net radiative and convective energy fluxes:

$$T(h, t + \Delta t) = T(h, t) + \frac{\Delta t}{c_p \rho}\left(\frac{dF_r}{dh} + \frac{dF_c}{dh}\right) \quad (4)$$

where c_p is the heat capacity at constant pressure, ρ the density of air, h the altitude, and dF_r/dh and dF_c/dh the net radiative and convective flux divergences. To compute dF_r/dh the radiative transfer equation is integrated over all frequencies, using the temperature profile of the previous time step and an assumed atmospheric composition. The term dF_c/dh is the energy transport needed to prevent the temperature gradient from exceeding a preassigned limit, usually 6.5°C km^{-1}. This limit parameterizes effects of vertical mixing and large-scale dynamics.

The radiative calculations are made by a method that groups absorption coefficients by strength for efficiency (*14*). Pressure- and temperature-dependent absorption coefficients are from line-by-line calculations for H_2O, CO_2, O_3, N_2O, and CH_4 (*15*), including continuum H_2O absorption (*16*). Climatological cloud cover (50 percent) and aerosol properties (*17*) are used, with appropriate fractions of low (0.3), middle (0.1), and high (0.1) clouds. Wavelength dependences of cloud and aerosol properties are obtained from Mie scattering theory (*14*). Multiple scattering and overlap of gaseous absorption bands are included. Our computations include the weak CO_2 bands at 8 to 12 μm, but the strong 15-μm CO_2 band, which closes one side of the 7- to 20-μm H_2O window, causes ≳ 90 percent of the CO_2 warming.

Model Sensitivity

We examine the main processes known to influence climate model sensitivity by inserting them individually into the model, as summarized in Table 1.

Model 1 has fixed absolute humidity, a fixed lapse rate of 6.5°C km^{-1} in the convective region, fixed cloud altitude, and no snow/ice albedo feedback or vegetation albedo feedback. The increase of equilibrium surface temperature for doubled atmospheric CO_2 is $\Delta T_s \sim 1.2$°C. This case is of special interest because it is the purely radiative-convective result, with no feedback effects.

Model 2 has fixed relative humidity, but is otherwise the same as model 1. The resulting ΔT_s for doubled CO_2 is ~1.9°C. Thus the increasing water vapor with higher temperature provides a feedback factor of ~1.6. Fixed relative humidity is clearly more realistic than fixed absolute humidity, as indicated by physical arguments (*13*) and three-dimensional model results (*7, 8*). Therefore, we use fixed relative humidity in the succeeding experiments and compare models 3 to 6 with model 2.

Model 3 has a moist adiabatic lapse rate in the convective region rather than a fixed lapse rate. This causes the equilibrium surface temperature to be less sensitive to radiative perturbations, and $\Delta T_s \sim 1.4$°C for doubled CO_2. The reason is that the lapse rate decreases as moisture is added to the air, reducing the temperature difference between the top of the convective region and the ground (ΓH in Eq. 3).

The general circulation of the earth's atmosphere is driven by solar heating of the tropical ocean, and resulting evaporation and vertical transport of energy. The lapse rate is nearly moist adiabatic at low latitudes and should remain so after a climate perturbation. Thus use of a moist adiabatic lapse rate is appropriate for the tropics. But more stable lapse rates at high latitudes make the surface temperature much more sensitive to perturbations of surface heating (*7, 8*), and hence model 3 would underestimate the sensitivity there.

Model 4 has the clouds at fixed temperature levels, and thus they move to a higher altitude as the temperature increases (*18*). This yields $\Delta T_s \sim 2.8$°C for doubled CO_2, compared to 1.9°C for fixed cloud altitude. The sensitivity increases because the outgoing thermal radiation from cloudy regions is defined by the fixed cloud temperature, requiring greater adjustment by the ground and lower atmosphere for outgoing radiation to balance absorbed solar radiation.

Study of Venus suggests that some clouds occur at a fixed temperature. The Venus cloud tops, which are the primary radiator to space, are at $H \sim 70$ km, where $T \sim T_e$. Analysis of the processes that determine the location of these clouds and the variety of clouds in the belts, zones, and polar regions on Jupiter should be informative. Available evidence suggests that the level of some terrestrial clouds depends on temperature while others occur at a fixed altitude. For example, tropical cirrus clouds moved to a higher altitude in the experiment of Hansen *et al.* (*8*) with doubled CO_2, but low clouds did not noticeably change altitude.

Models 5 and 6 illustrate snow/ice and vegetation albedo feedbacks (*19, 20*). Both feedbacks increase model sensitivity, since increased temperature decreases ground albedo and increases absorption of solar radiation.

Snow, sea ice, and land ice (ice sheets and glaciers) are all included in snow/ice albedo feedback. Snow and sea ice respond rapidly to temperature change, while continental ice sheets require thousands of years to respond. Thus a partial snow/ice albedo feedback is appropriate for time scales of 10 to 100 years. The vegetation albedo feedback was obtained by comparing today's global vegetation patterns with reconstruction of the Wisconsin ice age (*20*). Uncertainties in the

reconstruction, the time scale of vegetation response, and man's potential impact on vegetation prevent reliable assessment of this feedback, but its estimated magnitude emphasizes the need to monitor global vegetation and surface albedo.

Model 4 has our estimate of appropriate model sensitivity. The fixed 6.5°C km^{-1} lapse rate is a compromise between expected lower sensitivity at low latitudes and greater sensitivity at high latitudes. Both cloud temperature and snow/ice albedo feedback should be partly effective, so for simplicity one is included.

The sensitivity of the climate model we use is thus $\Delta T_s \sim 2.8$°C for doubled CO_2, similar to the sensitivity of three-dimensional climate models (*6–8*). The estimated uncertainty is a factor of 2. This sensitivity (i) refers to perturbations about today's climate and (ii) does not include feedback mechanisms effective only on long time scales, such as changes of ice sheets or ocean chemistry.

Table 1. Equilibrium surface temperature increase due to doubled CO_2 (from 300 to 600 ppm) in 1-D RC models. Model 1 has no feedbacks affecting the atmosphere's radiative properties. Feedback factor f specifies the effect of each added process on model sensitivity to doubled CO_2; F is the equilibrium thermal flux into the ground if T_s is held fixed (infinite heat capacity) when CO_2 is doubled. Abbreviations: FRH, fixed relative humidity; FAH, fixed absolute humidity; 6.5LR, 6.5°C km^{-1} limiting lapse rate; MALR, moist adiabatic limiting lapse rate; FCA, fixed cloud altitude, FCT, fixed cloud temperature; SAF, snow/ice albedo feedback; and VAF, vegetation albedo feedback. Models 5 and 6 are based on f values from Wang and Stone (*19*) and Cess (*20*), respectively, and ΔT_s of model 2.

Model	Description	ΔT_s (°C)	f	F (W m^{-2})
1	FAH, 6.5LR, FCA	1.22	1	4.0
2	FRH, 6.5LR, FCA	1.94	1.6	3.9
3	Same as 2, except MALR replaces 6.5LR	1.37	0.7	4.0
4	Same as 2, except FCT replaces FCA	2.78	1.4	3.9
5	Same as 2, except SAF included	2.5–2.8	1.3–1.4	
6	Same as 2, except VAF included	~3.5	~1.8	

Model Time Dependence

The time dependence of the earth's surface temperature depends on the heat capacity of the climate system. Heat capacity of land areas can be neglected, since ground is a good insulator. However, the upper 100 m of the ocean is rapidly mixed, so its heat capacity must be accounted for. The ocean beneath the mixed layer may also affect surface temperature, if the thermal response time of the mixed layer is comparable to the time for exchange of heat with deeper layers.

The great heat capacity of the ocean and ready exchange of continental and marine air imply that the global climate response to perturbations is determined by the response of the ocean areas. However, this response is affected by horizontal atmospheric heat fluxes from and to the continents. Ready exchange of energy between the ocean surface and atmosphere "fixes" the air temperature, and the ocean in effect removes from the atmosphere any net heat obtained from the continents. Thus the horizontal flux due to a climate perturbation's heating (or cooling) of the continents adds to the vertical heat flux into (or out of) the ocean surface. The net flux into the ocean surface is therefore larger than it would be for a 100 percent ocean-covered planet by the ratio of global area to ocean area, totaling ~5.7 W m^{-2} for doubled CO_2 rather than ~4 W m^{-2}. In a climate model that employs only a mixed-layer ocean, it is equivalent to use the flux ~4 W m^{-2} with the area-weighted mean land-ocean heat capacity.

The thermal response time of the ocean mixed layer would be ~3 years if it were not for feedback effects in the climate system. For example, assume that the solar flux absorbed by a planet changes suddenly from $F_0 \equiv \sigma T_0^4$ to $F_1 = F_0 + \Delta F \equiv \sigma T_1^4$, with $\Delta F << F_0$. The rate of change of heat in the climate system is

$$d(cT)/dt = \sigma T_1^4 - \sigma T^4 \quad (5)$$

where c is heat capacity per unit area. Since $T_1 - T_0 << T_0$, the solution is

$$T - T_1 = (T_0 - T_1)e^{-t/t_{thr}} \quad (6)$$

where

$$t_{thr} = c/4\sigma T_1^3 \quad (7)$$

Thus the planet approaches a new equilibrium temperature exponentially with e-folding time t_{thr}. If the heat capacity is provided by 70 m of water (100 m for ocean areas) and the effective temperature is 255 K, t_{thr} is 2.8 years.

This estimate does not account for climate feedback effects, which can be analyzed with the 1-D RC model. Table 1 shows that the initial rate of heat storage in the ocean is independent of feedbacks. Thus the time needed to reach equilibrium for model 4 is larger by the factor ~2.8°C/1.2°C than for model 1, which excludes feedbacks. The e-folding time for adjustment of mixed-layer temperature is therefore ~6 years for our best estimate of model sensitivity to doubled CO_2. This increase in thermal response time is readily understandable, because feedbacks come into play only gradually after some warming occurs.

It would take ~50 years to warm up the thermocline and mixed layer if they were rapidly mixed, or 250 years for the entire ocean. Turnover of the deep ocean, driven by formation of cold bottom water in the North Atlantic and Antarctic oceans with slow upwelling at low latitudes, is thought to require 500 to 1000 years (*21*), suggesting that the deep ocean does not greatly influence surface temperature sensitivity. However, there may be sufficient heat exchange between the mixed layer and thermocline to delay full impact of a climate perturbation by a few decades (*6, 22, 23*). The primary mechanism of exchange is nearly horizontal movement of water along surfaces of constant density (*21*).

Delay of CO_2 warming by the ocean can be illustrated with a "box diffusion" model (*24*), in which heat is stirred instantly through the mixed layer and diffused into the thermocline with diffusion coefficient k. Observed oceanic penetration by inert chemical tracers suggests that k is of order 1 square centimeter per second (*2, 3, 24*).

The warming calculated with the one-dimensional model for the CO_2 increase from 1880 to 1980 (*25*) is 0.5°C if ocean heat capacity is neglected (Fig. 1). The heat capacity of just the mixed layer reduces this to 0.4°C, a direct effect of the mixed layer's 6-year thermal response time. Diffusion into the thermocline further reduces the warming to 0.25°C for $k = 1$ cm^2 sec^{-1}, an indirect effect of the mixed layer's 6-year e-folding time, which permits substantial exchange with the thermocline.

The mixed-layer model and thermocline model bracket the likely CO_2 warming. The thermocline model is preferable for small climate perturbations that do not affect ocean mixing. However, one effect of warming the ocean surface will be increased vertical stability, which could reduce ocean warming and make the surface temperature response more like that of the mixed-layer case.

Lack of knowledge of ocean processes

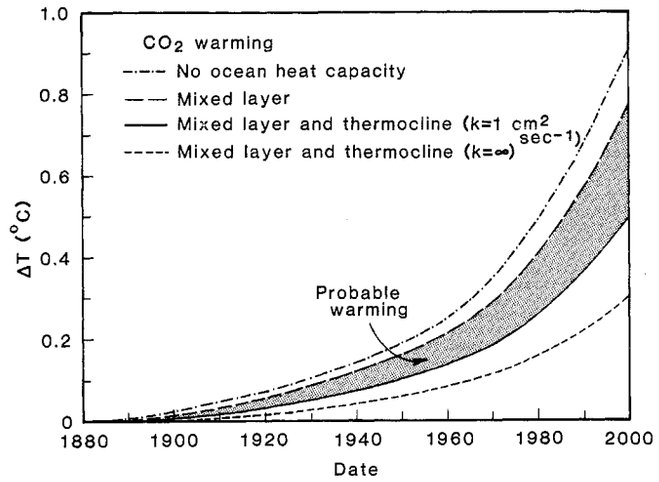

Fig. 1. Dependence of CO_2 warming on ocean heat capacity. Heat is rapidly mixed in the upper 100 m of the ocean and diffused to 1000 m with diffusion coefficient k. The CO_2 abundance, from (*25*), is 293 ppm in 1880, 335 ppm in 1980, and 373 ppm in 2000. Climate model equilibrium sensitivity is 2.8°C for doubled CO_2.

primarily introduces uncertainties about the time dependence of the global CO_2 warming. The full impact of the warming may be delayed several decades, but since man-made increases in atmospheric CO_2 are expected to persist for centuries (*1, 2, 6*), the warming will eventually occur.

Radiative Climate Perturbations

Identification of the CO_2 warming in observed climate depends on the magnitude of climate variability due to other factors. Most suspected causes of global climate change are radiative perturbations, which can be compared to identify those capable of counteracting or reinforcing the CO_2 warming.

A 1 percent increase of solar luminosity would warm the earth 1.6°C at equilibrium (Fig. 2) on the basis of model 4, which we employ for all radiative perturbations to provide a uniform comparison. Since the effect is linear for small changes of solar luminosity, a change of 0.3 percent would modify the equilibrium global mean temperature by 0.5°C, which is as large as the equilibrium warming for the cumulative increase of atmospheric CO_2 from 1880 to 1980. Solar luminosity variations of a few tenths of 1 percent could not be reliably measured with the techniques available during the past century, and thus are a possible cause of part of the climate variability in that period.

Atmospheric aerosol effects depend on aerosol composition, size, altitude, and global distribution (*26*). Based on model calculations, stratospheric aerosols that persist for 1 to 3 years after large volcanic eruptions can cause substantial cooling of surface air (Fig. 2). The cooling depends on the assumption that the particles do not exceed a few tenths of a micrometer in size, so they do not cause greenhouse warming by blocking terrestrial radiation, but this condition is probably ensured by rapid gravitational settling of larger particles. Temporal variability of stratospheric aerosols due to volcanic eruptions appears to have been responsible for a large part of the observed climate change during the past century (*27–30*), as shown below.

The impact of tropospheric aerosols on climate is uncertain in sense and magnitude due to their range of composition, including absorbing material such as carbon and high-albedo material such as sulfuric acid, and their heterogeneous spatial distribution. Although man-made tropospheric aerosols are obvious near their source, aerosol opacity does not appear to have increased much in remote regions (*31*). Since the climate impact of anthropogenic aerosols is also reduced by the opposing effects of absorbing and high-albedo materials, it is possible that they have not had a primary effect on global temperature. However, global monitoring of aerosol properties is needed for conclusive analysis.

Ground albedo alterations associated with changing patterns of vegetation coverage have been suggested as a cause of global climate variations on time scales of decades to centuries (*32*). A global surface albedo change of 0.015, equivalent to a change of 0.05 over land areas, would affect global temperature by 1.3°C. Since this is a 25 percent change in mean continental ground albedo, it seems unlikely that ground albedo variations have been the primary cause of recent global temperature trends. However, global monitoring of ground albedo is needed to permit definitive assessment of its role in climate variability.

High and low clouds have opposite effects on surface temperature (Fig. 2), high clouds having a greenhouse effect while low clouds cool the surface (*14, 33*). However, the nature and causes of variability of cloud cover, optical thickness, and altitude distribution are not well known, nor is it known how to model reliably cloud feedbacks that may occur in response to climate perturbations. Progress may be made after accurate cloud climatology is obtained from global observations, including seasonal and interannual cloud variations. In the

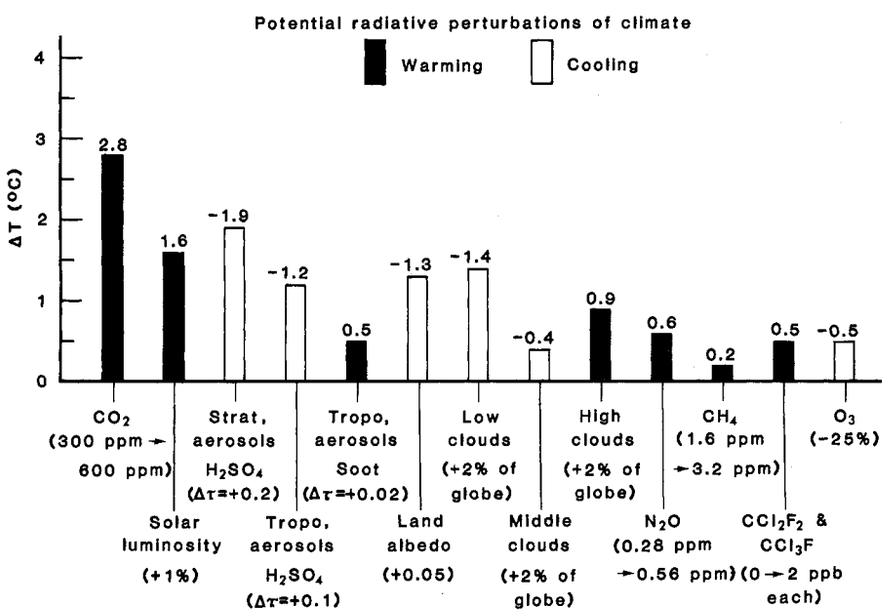

Fig. 2. Surface temperature effect of various global radiative perturbations, based on the 1-D RC model 4 (Table 1). Aerosols have the physical properties specified by (*17*). Dependence of ΔT on aerosol size, composition, altitude, and optical thickness is illustrated by (*26*). The $\Delta\tau$ for stratospheric aerosols is representative of a very large volcanic eruption.

meantime, some limits are implicitly placed on global cloud feedback by empirical tests of the climate system's sensitivity to radiative perturbations, as discussed below.

Trace gases that absorb in the infrared can warm the earth if their abundance increases (*5, 34*). The abundance of chlorofluorocarbons (Freons) increased from a negligible amount a few decades ago to 0.3 part per billion for CCl_2F_2 and 0.2 ppb for CCl_3F (*35*), with an equilibrium greenhouse warming of ~ 0.06°C. Recent measurement of a 0.2 percent per year increase of N_2O suggests a cumulative increase to date of 17 ppb (*36*), with an equilibrium warming of ~ 0.03°C. Tentative indications of a 2 percent per year increase in CH_4 imply an equilibrium warming < 0.1°C for the CH_4 increase to date (*37*). No major trend of O_3 abundance has been observed, although it has been argued that continued increase of Freons will reduce O_3 amounts (*38*). The net impact of measured trace gases has thus been an equilibrium warming of 0.1°C or slightly larger. This does not greatly alter analyses of temperature change over the past century, but trace gases will significantly enhance future greenhouse warming if recent growth rates are maintained.

We conclude that study of global climate change on time scales of decades and centuries must consider variability of stratospheric aerosols and solar luminosity, in addition to CO_2 and trace gases. Tropospheric aerosols and ground albedo are potentially significant, but require better observations. Cloud variability will continue to cause uncertainty until accurate monitoring of global cloud properties provides a basis for realistic modeling of cloud feedback effects; however, global feedback is implicitly checked by comparison of climate model sensitivity to empirical climate variations, as done below.

Observed Temperature Trends

Data archives (*39*) contain surface air temperatures of several hundred stations for the last century. Problems in obtaining a global temperature history are due to the uneven station distribution (*40*), with the Southern Hemisphere and ocean areas poorly represented, and the smaller number of stations for earlier times.

We combined these temperature records with a method designed to extract mean temperature trends. The globe was divided by grids with a spacing not larger than the correlation distance for primary dynamical transports (*41*), but large enough that most boxes contained one or more stations. The results shown were obtained with 40 equal-area boxes in each hemisphere, but the conclusions are not sensitive to the exact spacing. Temperature trends for stations within a box were combined successively:

$$T_{1,n}(t) = \frac{(n^* - 1)T_{1,n} + T_n - \bar{T}_n + \bar{T}_{1,n}}{n^*} \quad (8)$$

to obtain a single trend for each box, where the bar indicates a mean for the years in which there are records for both T_n and the cumulative $T_{1,n}$ and $n^*(t)$ is the number of stations in $T_{1,n}(t)$. Trends for boxes in a latitude zone were combined with each box weighted equally, and the global trend was obtained by area-weighting the trends for all latitude zones. A meaningful result begins in the 1880's, since thereafter continuous records exist for at least two widely separated longitudes in seven of the eight latitude zones (continuous Antarctic temperatures begin in the 1950's). Results are least reliable for 1880 to 1900; by 1900, continuous records exist for more than half of the 80 boxes.

The temperature trends in Fig. 3 are smoothed with a 5-year running mean to make the trends readily visible. Part of the noise in the unsmoothed data results from unpredictable weather fluctuations, which affect even 1-year means (*42*). None of our conclusions depends on the nature of the smoothing.

Northern latitudes warmed ~ 0.8°C between the 1880's and 1940, then cooled ~ 0.5°C between 1940 and 1970, in agreement with other analyses (*9, 43*). Low latitudes warmed ~ 0.3°C between 1880 and 1930, with little change thereafter. Southern latitudes warmed ~ 0.4°C in the past century; results agree with a prior analysis for the late 1950's to middle 1970's (*44*). The global mean temperature increased ~ 0.5°C between 1885 and 1940, with slight cooling thereafter.

A remarkable conclusion from Fig. 3 is that the global temperature is almost as high today as it was in 1940. The common misconception that the world is cooling is based on Northern Hemisphere experience to 1970.

Another conclusion is that global surface air temperature rose ~ 0.4°C in the past century, roughly consistent with calculated CO_2 warming. The time history of the warming obviously does not follow the course of the CO_2 increase (Fig. 1), indicating that other factors must affect global mean temperature.

Model Verification

Natural radiative perturbations of the earth's climate, such as those due to aerosols produced by large volcanic

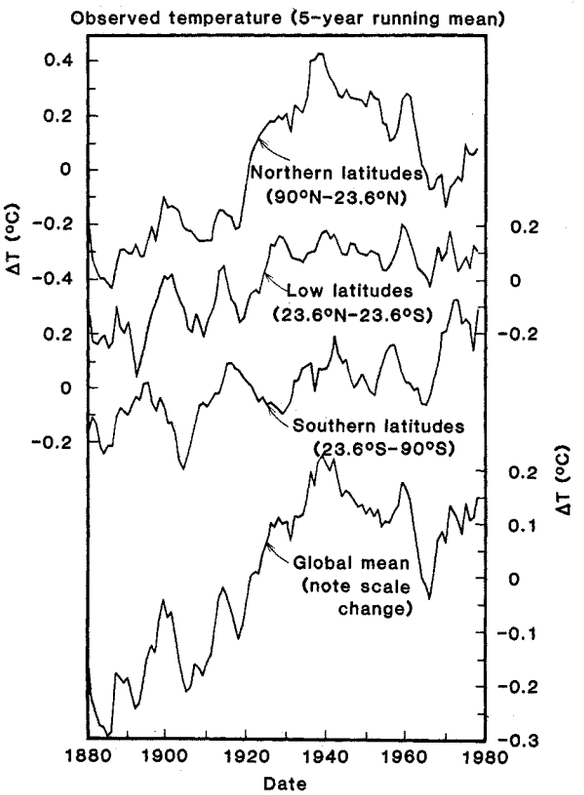

Fig. 3. Observed surface air temperature trends for three latitude bands and the entire globe. Temperature scales for low latitudes and global mean are on the right.

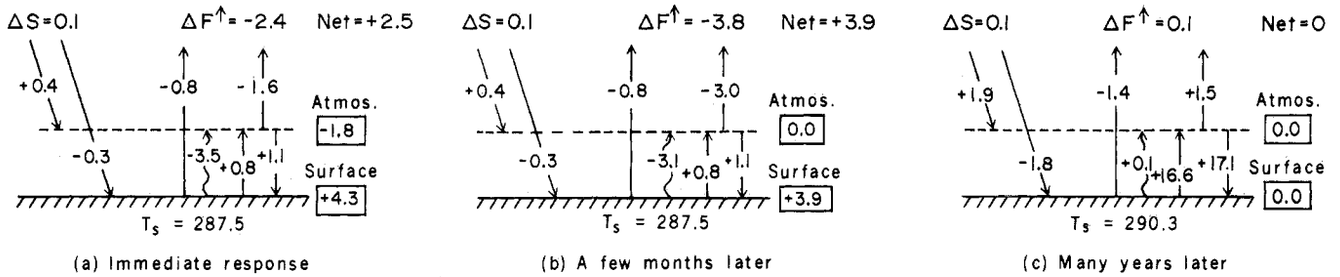

Fig. 4. Change of fluxes (watts per square meter) in the 1-D RC model when atmospheric CO_2 is doubled (from 300 to 600 ppm). Symbols: ΔS, change in solar radiation absorbed by the atmosphere and surface; $\Delta F\uparrow$, change in outward thermal radiation at top of the atmosphere. The wavy line represents convective flux; other fluxes are radiative.

eruptions, permit a valuable test of model sensitivity. Previous study of the best-documented large volcanic eruption, Mount Agung in 1963, showed that tropical tropospheric and stratospheric temperature changes computed with a one-dimensional climate model were of the same sign and order of magnitude as observed changes (*45*). It was assumed that horizontal heat exchange with higher latitudes was not altered by the radiative perturbation.

We reexamined the Mount Agung case for comparison with the present global temperature record, using our model with sensitivity ~ 2.8°C. The model, with a maximum global mean aerosol increase in the optical depth $\Delta\tau = 0.12$ (*45*), yields a maximum global cooling of 0.2°C when only the mixed-layer heat capacity is included and 0.1°C when heat exchange with the deeper ocean is included with $k = 1$ cm^2 sec^{-1}. Observations suggest a cooling of this magnitude with the expected time lag of 1 to 2 years. Noise or unexplained variability in the observations prevents more definitive conclusions, but similar cooling is indicated by statistical studies of temperature trends following other large volcanic eruptions (*46*).

A primary lesson from the Mount Agung test is the damping of temperature change by the mixed layer's heat capacity, without which the cooling would have exceeded 1.1°C (Fig. 2). The effect can be understood from the time constant of the perturbation and thermal response time of the mixed layer: $\Delta T \sim \{1 - \exp[(-1\text{ year})/(6\text{ years})]\} \times 1.1°C \sim 0.17°C$, for the case $k = 0$. This large reduction of the climate response occurs for a perturbation that (unlike CO_2) is present for a time shorter than the thermal response time of the ocean surface.

Phenomena that alter the regional radiation balance provide another model test. Idso (*11*) found a consistent "empirical response function" for several such phenomena, which was 0.17°C per watt per square meter in midcontinent and was half as large on the coast. This response must depend on the rate of mixing of marine and continental air, since the phenomena occur on time scales less than the thermal relaxation time of the ocean surface. Thus, as one test of horizontal atmospheric transports, we read from our three-dimensional climate model (*8*) the quantities (solar insolation and temperature) that form Idso's empirical response function for seasonal change of insolation. Results ranged from 0.2°C W^{-1} m^2 in midcontinent, and about half that on the coast, to a value an order of magnitude smaller over the ocean, in agreement with the empirical response (*11*).

To relate these empirical tests to the CO_2 greenhouse effect, we illustrate the flux changes in the 1-D RC model when CO_2 is doubled. For simplicity we consider an instantaneous doubling of CO_2, and hence the time dependence of the response does not represent the transient response to a steady change in CO_2. The immediate response to the doubling includes (Fig. 4a): (i) reduced emission to space (− 2.4 W m^{-2}), because added CO_2 absorption raises the mean altitude of emission to a higher, colder level; (ii) increased flux from atmosphere to ground (+ 1.1 W m^{-2}); and (iii) increased stratospheric cooling but decreased tropospheric cooling. The radiative warming of the troposphere decreases the "convective" flux (latent and sensible heat) from the ground by 3.5 W m^{-2} as a consequence of the requirement to conserve energy. There is a small increase in absorption of near-infrared radiation, the atmosphere gaining energy (+ 0.4 W m^{-2}) and the ground losing energy (− 0.3 W m^{-2}). The net effect is thus an energy gain for the planet (+ 2.5 W m^{-2}) with heating of the ground (+ 4.3 W m^{-2}) and cooling of the (upper) atmosphere (− 1.8 W m^{-2}). These flux changes are independent of feedbacks and are not sensitive to the critical lapse rate.

A few months after the CO_2 doubling (Fig. 4b) the stratospheric temperature has cooled by ~ 5°C. Neither the ocean nor the troposphere, which is convectively coupled to the surface, have responded yet. The planet radiates 3.8 W m^{-2} less energy to space than in the comparison case with 300 ppm CO_2, because of the cooler stratosphere and greater altitude of emission from the troposphere. The energy gained by the earth at this time is being used to warm the ocean.

Years later (Fig. 4c) the surface temperature has increased 2.8°C. Almost half the increase (1.2°C) is the direct CO_2 greenhouse effect. The remainder is due to feedbacks, of which 1.0°C is the well-established H_2O greenhouse effect.

The greenhouse process represented in Fig. 4 is simply the "leaky bucket" phenomenon. The increased infrared opacity causes an immediate decrease of thermal radiation from the planet, thus forcing the temperature to rise until energy balance is restored. Temporal variations of the fluxes and temperatures are due to the response times of the atmosphere and surface.

Surface warming of ~ 3°C for doubled CO_2 is the status after energy balance has been restored. This contrasts with the Agung case and the cases considered by Idso (*11*), which are all nonequilibrium situations.

The test of the greenhouse theory provided by the extremes of equilibrium climates on the planets and short-term radiative perturbations is reassuring, but inadequate. A crucial intermediate test is climate change on time scales from a few years to a century.

Model versus Observations for the Past Century

Simulations of global temperature change should begin with the known forcings: variations of CO_2 and volcanic aerosols. Solar luminosity variations, which constitute another likely mecha-

nism, are unknown, but there are hypotheses consistent with observational constraints that variations not exceed a few tenths of 1 percent.

We developed an empirical equation that fits the heat flux into the earth's surface calculated with the 1-D RC climate model (model 4):

$$F(t) = 0.018\Delta p/(1 + 0.0022\Delta p)^{0.6} - 17\Delta\tau - 1.5(\Delta\tau)^2 + 220\Delta S/S_0 - 1.5\Delta T + 0.033\,(\Delta T)^2 - 1.04 \times 10^{-4}\Delta p\Delta T + 0.29\Delta T\Delta\tau \quad (9)$$

where $F(t)$ is in watts per square meter, p is the amount of CO_2 in parts per million above an "equilibrium" value (293 ppm), ΔS is the difference between solar luminosity and an equilibrium value S_0, $\Delta\tau$ is the optical depth of stratospheric aerosols above a background amount, and ΔT is the difference between current surface temperature and the equilibrium value for $\Delta p = \Delta S = \Delta\tau = 0$. Equation 9 fits the one-dimensional model results to better than 1 percent for $0 \leq \Delta p \leq 1200$ ppm, $0.98 \leq \Delta S/S_0 \leq 1.02$, and $\Delta\tau \leq 0.5$. For the mixed-layer ocean model $T_s(t)$ follows from $dT_s/dt = F(t)/c_0$, where c_0 is the heat capacity of the ocean mixed layer per unit area. If the true mixed-layer depth is used to obtain c_0, $F(t)$ must be multiplied by 1/0.7, the ratio of global area to ocean area. Diffusion of heat into the deeper ocean can then also be included by means of the diffusion equation with T_s as its upper boundary condition.

The CO_2 abundance increased from 293 ppm in 1880 to 335 ppm in 1980 (*25*), based on recent accurate observations, earlier less accurate observations, and carbon cycle modeling. The error for 1880 probably does not exceed 10 ppm (*1, 2*).

Volcanic aerosol radiative forcing can be obtained from Lamb's (*27*) dust veil index (DVI), which is based mainly on atmospheric transmission measurements after 1880. We convert DVI to optical depth by taking Mount Agung (DVI = 800) to have the maximum $\Delta\tau = 0.12$. The aerosol optical depth histories of Mitchell (*47*) and Pollack *et al.* (*29*), the latter based solely on transmission measurements, are similar to Lamb's. We use aerosol microphysical properties from (*45*). The error in volcanic aerosol radiative forcing probably does not exceed a factor of 2.

Solar variability is highly conjectural, so we first study CO_2 and volcanic aerosol forcings and then add solar variations. We examine the hypothesis of Hoyt (*48*) that the ratio, r, of umbra to penumbra areas in sunspots is proportional to solar luminosity: $\Delta S/S_0 = f(r - r_0)$. Hoyt's rationale is that the penumbra, with a weaker magnetic field than the umbra, is destroyed more readily by an increase of convective flux from below. We take $f = 0.03$, which implies a peak-to-peak amplitude of ~ 0.4 percent for $\Delta S/S_0$ in the past century, or an amplitude of ~ 0.2 percent for the mean trend line. Taking S_0 as the mean for 1880 to 1976 yields $r_0 = 0.2$. The resulting $\Delta S/S_0$ has no observational corroboration, but serves as an example of solar variability of a plausible magnitude.

Radiative forcing by CO_2 plus volcanoes and forcing by CO_2 plus volcanoes plus the sun both yield a temperature trend with a strong similarity to the observed trend of the past century (Fig. 5), which we quantify below. If only the heat capacity of the mixed layer is included, the amplitude of the computed temperature variations is larger than observed. However, mixing of heat into the deeper ocean with $k = 1$ cm^2 sec^{-1} brings both calculated trends into rough agreement with observations.

The main uncertainties in the climate model—that is, its "tuning knobs"—are (i) the equilibrium sensitivity and (ii) the rate of heat exchange with the ocean beneath the mixed layer. The general correlation of radiative forcings with global temperatures suggests that model uncertainties be constrained by requiring agreement with the observed temperature trend.

Therefore, we examined a range of model sensitivities, choosing a diffusion coefficient for each to minimize the residual variance between computed and observed temperature trends. Equilibrium sensitivities of 1.4°, 2.8°, and 5.6°C required $k = 0$, 1.2, and 2.2 cm^2 sec^{-1}, respectively. All models with sensitivities of 1.4° to 5.6°C provide a good fit to the observations. The smallest acceptable sensitivity is ~ 1.4°C, because it requires zero heat exchange with the deeper ocean. Sensitivities much higher than 5.6°C would require greater heat exchange with the deep ocean than is believed to be realistic (*21, 22*).

Radiative forcing by CO_2 plus volcanoes accounts for 75 percent of the variance in the 5-year smoothed global temperature, with correlation coefficient 0.9. The hypothesized solar luminosity variation (*48*) improves the fit, as a consequence of the luminosity peaking in the 1930's and declining into the 1970's, leaving a residual variance of only 10 percent. The improved fit provided by Hoyt's solar variability represents a posteriori selection, since other hypothesized solar variations that we examined [for instance (*49*)] degrade the fit. This

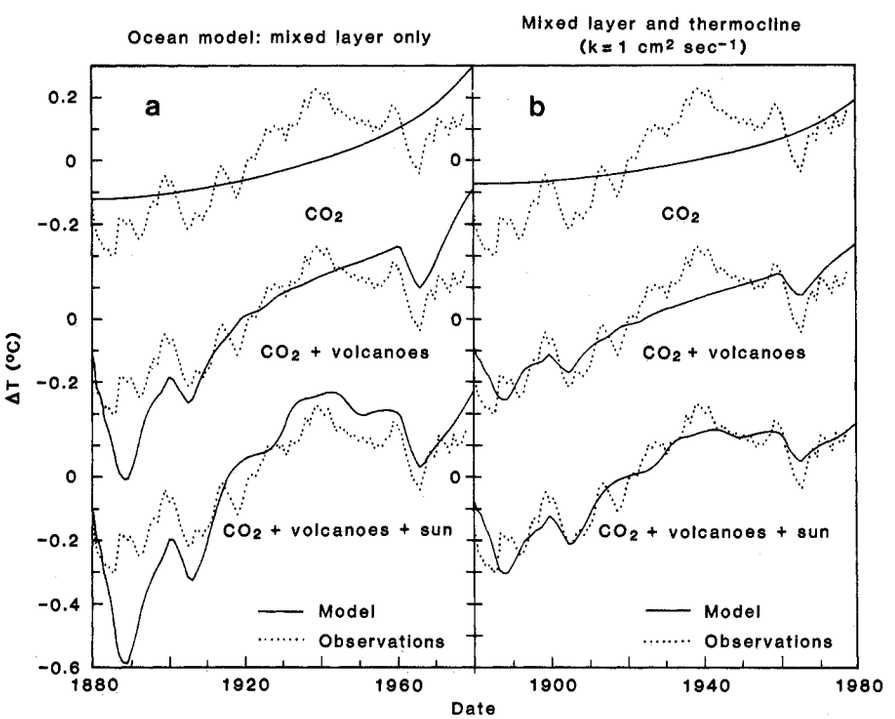

Fig. 5. Global temperature trend obtained from climate model with sensitivity 2.8°C for doubled CO_2. The results in (a) are based on a 100-m mixed-layer ocean for heat capacity; those in (b) include diffusion of heat into the thermocline to 1000 m. The forcings by CO_2, volcanoes, and the sun are based on Broecker (*25*), Lamb (*27*), and Hoyt (*48*). Mean ΔT is zero for observations and model.

Table 2. Energy supplied and CO_2 released by fuels.

Fuel	Energy supplied in 1980*		CO_2 release per unit energy (oil = 1)	Airborne CO_2 added in 1980*		CO_2 added through 1980 (ppm)	Potential airborne CO_2 in virgin reservoirs† (ppm)
	(10^{19} J)	(%)		(%)	(ppm)		
Oil	12	40	1	50	0.7	11	70
Coal	7	24	5/4	35	0.5	26	1000
Gas	5	16	3/4	15	0.2	5	50
Oil shale, tar sands, heavy oil	0	0	7/4	0	0	0	100
Nuclear, solar, wood, hydroelectric	6	20	0	0	0	0	0
Total	30	100		100	1.4	42	1220

*Based on late 1970's. †Reservoir estimates assume that half the coal above 3000 feet can be recovered and that oil recovery rates will increase from 25 to 30 percent to 40 percent. Estimate for unconventional fossil fuels may be low if techniques are developed for economic extraction of "synthetic oil" from deposits that are deep or of marginal energy content. It is assumed that the airborne fraction of released CO_2 is fixed.

evidence is too weak to support any specific solar variability.

The general agreement between modeled and observed temperature trends strongly suggests that CO_2 and volcanic aerosols are responsible for much of the global temperature variation in the past century. Key consequences are: (i) empirical evidence that much of the global climate variability on time scales of decades to centuries is deterministic and (ii) improved confidence in the ability of models to predict future CO_2 climate effects.

Projections into the 21st Century

Prediction of the climate effect of CO_2 requires projections of the amount of atmospheric CO_2, which we specify by (i) the energy growth rate and (ii) the fossil fuel proportion of energy use. We neglect other possible variables, such as changes in the amount of biomass or the fraction of released CO_2 taken up by the ocean.

Energy growth has been 4 to 5 percent per year in the past century, but increasing costs will constrain future growth (*1*, *4*). Thus we consider fast growth (~ 3 percent per year, specifically 4 percent per year in 1980 to 2020, 3 percent per year in 2020 to 2060, and 2 percent per year in 2060 to 2100), slow growth (half of fast growth), and no growth as representative energy growth rates.

Fossil fuel use will be limited by available resources (Table 2). Full use of oil and gas will increase CO_2 abundance by < 50 percent of the preindustrial amount. Oil and gas depletion are near the 25 percent level, at which use of a resource normally begins to be limited by supply and demand forces (*4*). But coal, only 2 to 3 percent depleted, will not be so constrained for several decades.

The key fuel choice is between coal and alternatives that do not increase atmospheric CO_2. We examine a synfuel option in which coal-derived synthetic fuels replace oil and gas as the latter are depleted, and a nuclear/renewable resources option in which the replacement fuels do not increase CO_2. We also examine a coal phaseout scenario: after a specific date coal and synfuel use are held constant for 20 years and then phased out linearly over 20 years.

Projected global warming for fast growth is 3° to 4.5°C at the end of the next century, depending on the proportion of depleted oil and gas replaced by synfuels (Fig. 6). Slow growth, with depleted oil and gas replaced equally by synfuels and nonfossil fuels, reduces the warming to ~ 2.5°C. The warming is only slightly more than 1°C for either (i) no energy growth, with depleted oil and gas replaced by nonfossil fuels, or (ii) slow energy growth, with coal and synfuels phased out beginning in 2000.

Other climate forcings may counteract or reinforce CO_2 warming. A decrease of solar luminosity from 1980 to 2100 by 0.6 percent per century, large compared to measured variations, would decrease the warming ~ 0.7°C. Thus CO_2 growth as large as in the slow-growth scenario would overwhelm the effect of likely solar variability. The same is true of other radiative perturbations; for instance, volcanic aerosols may slow the rise in temperature, but even an optical thickness of 0.1 maintained for 120 years would reduce the warming by less than 1.0°C.

When should the CO_2 warming rise out of the noise level of natural climate variability? An estimate can be obtained by comparing the predicted warming to the standard deviation, σ, of the observed global temperature trend of the past century (*50*). The standard deviation, which increases from 0.1°C for 10-year intervals to 0.2°C for the full century, is the total variability of global temperature; it thus includes variations due to any known radiative forcing, other variations of the true global temperature due to unidentified causes, and noise due to imperfect measurement of the global temperature. Thus if T_0 is the current 5-year smoothed global temperature, the 5-year smoothed global temperature in 10 years should be in the range $T_0 \pm 0.1$°C with probability ~ 70 percent, judging only from variability in the past century.

The predicted CO_2 warming rises out of the 1σ noise level in the 1980's and the 2σ level in the 1990's (Fig. 7). This is independent of the climate model's equilibrium sensitivity for the range of likely values, 1.4° to 5.6°C. Furthermore, it does not depend on the scenario for atmospheric CO_2 growth, because the amounts of CO_2 do not differ substantially until after year 2000. Volcanic eruptions of the size of Krakatoa or Agung may slow the warming, but barring an unusual coincidence of eruptions, the delay will not exceed several years.

Nominal confidence in the CO_2 theory will reach ~ 85 percent when the temperature rises through the 1σ level and ~ 98 percent when it exceeds 2σ. However, a portion of σ may be accounted for in the future from accurate knowledge of some radiative forcings and more precise knowledge of global temperature. We conclude that CO_2 warming should rise above the noise level of natural climate variability in this century.

Potential Consequences of Global Warming

Practical implications of CO_2 warming can only be crudely estimated, based on climate models and study of past climate. Models do not yet accurately simulate many parts of the climate system, especially the ocean, clouds, polar sea ice, and ice sheets. Evidence from past climate is also limited, since the few recent warm periods were not as extreme as the warming projected to accompany full use of fossil fuels, and the climate forcings and rate of climate change may have been different. However, if checked against our understanding of the physical processes and used with caution, the models and data on past climate provide useful indications of possible future climate effects (*51*).

Paleoclimatic evidence suggests that surface warming at high latitudes will be two to five times the global mean warming (*52–55*). Climate models predict the

larger sensitivity at high latitudes and trace it to snow/ice albedo feedback and greater atmospheric stability, which magnifies the warming of near-surface layers (*6–8*). Since these mechanisms will operate even with the expected rapidity of CO_2 warming, it can be anticipated that average high-latitude warming will be a few times greater than the global mean effect.

Climate models indicate that large regional climate variations will accompany global warming. Such shifting of climatic patterns has great practical significance, because the precipitation patterns determine the locations of deserts, fertile areas, and marginal lands. A major regional change in the doubled CO_2 experiment with our three-dimensional model (*6, 8*) was the creation of hot, dry conditions in much of the western two-thirds of the United States and Canada and in large parts of central Asia. The hot, dry summer of 1980 may be typical of the United States in the next century if the model results are correct. However, the model shows that many other places, especially coastal areas, are wetter with doubled CO_2.

Reconstructions of regional climate patterns in the altithermal (*53, 54*) show some similarity to these model results. The United States was drier than today during that warm period, but most regions were wetter than at present. For example, the climate in much of North Africa and the Middle East was more favorable for agriculture 8000 to 4000 years ago, at the time civilization dawned in that region.

Beneficial effects of CO_2 warming will include increased length of the growing season. It is not obvious whether the world will be more or less able to feed its population. Major modifications of regional climate patterns will require efforts to readjust land use and crop characteristics and may cause large-scale human dislocations. Improved global climate models, reconstructions of past climate, and detailed analyses are needed before one can predict whether the net long-term impact will be beneficial or detrimental.

Melting of the world's ice sheets is another possible effect of CO_2 warming. If they melted entirely, sea level would rise ~ 70 m. However, their natural response time is thousands of years, and it is not certain whether CO_2 warming will cause the ice sheets to shrink or grow. For example, if the ocean warms but the air above the ice sheets remains below freezing, the effect could be increased snowfall, net ice sheet growth, and thus lowering of sea level.

Danger of rapid sea level rise is posed by the West Antarctic ice sheet, which, unlike the land-based Greenland and East Antarctic ice sheets, is grounded below sea level, making it vulnerable to rapid disintegration and melting in case of general warming (*55*). The summer temperature in its vicinity is about −5°C. If this temperature rises ~ 5°C, deglaciation could be rapid, requiring a century or less and causing a sea level rise of 5 to 6 m (*55*). If the West Antarctic ice sheet melts on such a time scale, it will temporarily overwhelm any sea level change due to growth or decay of land-based ice sheets. A sea level rise of 5 m would flood 25 percent of Louisiana and Florida, 10 percent of New Jersey, and many other lowlands throughout the world.

Climate models (*7, 8*) indicate that ~ 2°C global warming is needed to cause ~ 5°C warming at the West Antarctic ice sheet. A 2°C global warming is exceeded in the 21st century in all the CO_2 scenarios we considered, except no growth and coal phaseout.

Floating polar sea ice responds rapidly to climate change. The 5° to 10°C warming expected at high northern latitudes for doubled CO_2 should open the North-

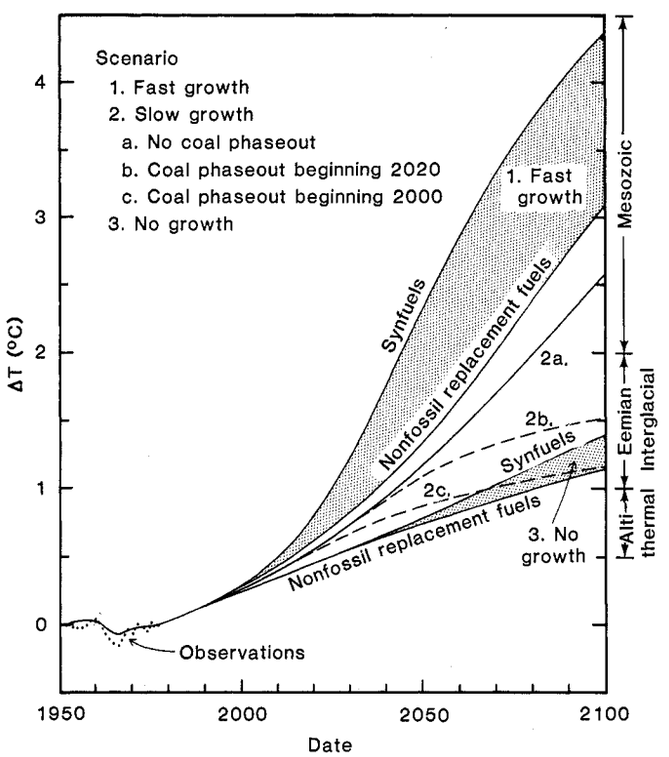

Fig. 6. Projections of global temperature. The diffusion coefficient beneath the ocean mixed layer is 1.2 cm^2 sec^{-1}, as required for best fit of the model and observations for the period 1880 to 1978. Estimated global mean warming in earlier warm periods is indicated on the right.

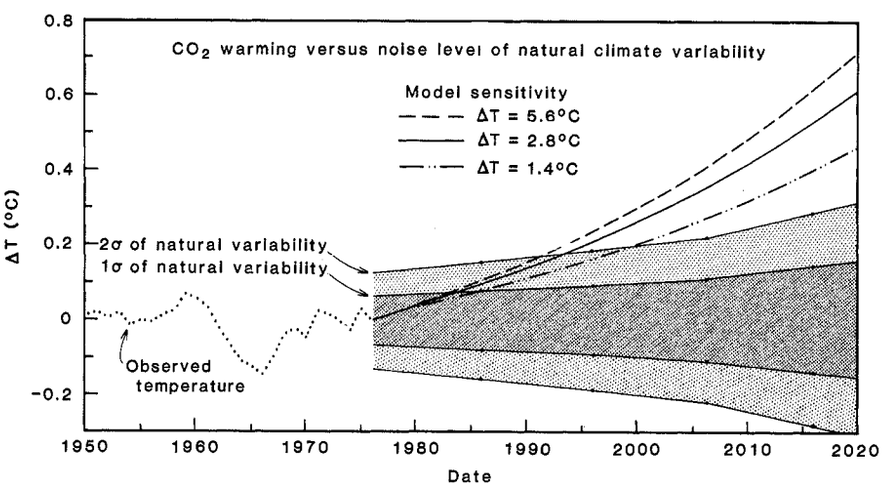

Fig. 7. Comparison of projected CO_2 warming to standard deviation (σ) of observed global temperature and to 2σ. The standard deviation was computed for the observed global temperatures in Fig. 3. Carbon dioxide change is from the slow-growth scenario. The effect of other trace gases is not included.

west and Northeast passages along the borders of the American and Eurasian continents. Preliminary experiments with sea ice models (*56*) suggest that all the sea ice may melt in summer, but part of it would refreeze in winter. Even a partially ice-free Arctic will modify neighboring continental climates.

Discussion

The global warming projected for the next century is of almost unprecedented magnitude. On the basis of our model calculations, we estimate it to be ~ 2.5°C for a scenario with slow energy growth and a mixture of nonfossil and fossil fuels. This would exceed the temperature during the altithermal (6000 years ago) and the previous (Eemian) interglacial period 125,000 years ago (*53*), and would approach the warmth of the Mesozoic, the age of dinosaurs.

Many caveats must accompany the projected climate effects. First, the increase of atmospheric CO_2 depends on the assumed energy growth rate, the proportion of energy derived from fossil fuels, and the assumption that about 50 percent of anthropogenic CO_2 emissions will remain airborne. Second, the predicted global warming for a given CO_2 increase is based on rudimentary abilities to model a complex climate system with many nonlinear processes. Tests of model sensitivity, ranging from the equilibrium climates on the planets to perturbations of the earth's climate, are encouraging, but more tests are needed. Third, only crude estimates exist for regional climate effects.

More observations and theoretical work are needed to permit firm identification of the CO_2 warming and reliable prediction of larger climate effects farther in the future. It is necessary to monitor primary global radiative forcings: solar luminosity, cloud properties, aerosol properties, ground albedo, and trace gases. Exciting capabilities are within reach. For example, the NASA Solar Maximum Mission is monitoring solar output with a relative accuracy of ~ 0.01 percent (*57*). Studies of certain components of the climate system are needed, especially heat storage and transport by the oceans and ice sheet dynamics. These studies will require global monitoring and local measurements of processes, guided by theoretical studies. Climate models must be developed to reliably simulate regional climate, including the transient response (*58*) to gradually increasing CO_2 amount.

Political and economic forces affecting energy use and fuel choice make it unlikely that the CO_2 issue will have a major impact on energy policies until convincing observations of the global warming are in hand. In light of historical evidence that it takes several decades to complete a major change in fuel use, this makes large climate change almost inevitable. However, the degree of warming will depend strongly on the energy growth rate and choice of fuels for the next century. Thus, CO_2 effects on climate may make full exploitation of coal resources undesirable. An appropriate strategy may be to encourage energy conservation and develop alternative energy sources, while using fossil fuels as necessary during the next few decades.

The climate change induced by anthropogenic release of CO_2 is likely to be the most fascinating global geophysical experiment that man will ever conduct. The scientific task is to help determine the nature of future climatic effects as early as possible. The required efforts in global observations and climate analysis are challenging, but the benefits from improved understanding of climate will surely warrant the work invested.

References and Notes

1. National Academy of Sciences, *Energy and Climate* (Washington, D.C., 1977).
2. U. Siegenthaler and H. Oeschger, *Science* **199**, 388 (1978).
3. W. S. Broecker, T. Takahashi, H. J. Simpson, T.-H. Peng, *ibid.* **206**, 409 (1979).
4. R. M. Rotty and G. Marland, *Oak Ridge Assoc. Univ. Rep. IEA-80-9(M)* (1980).
5. W. C. Wang, Y. L. Yung, A. A. Lacis, T. Mo, J. E. Hansen, *Science* **194**, 685 (1976).
6. National Academy of Sciences, *Carbon Dioxide and Climate: A Scientific Assessment* (Washington, D.C., 1979). This report relies heavily on simulations made with two three-dimensional climate models (*7, 8*) that include realistic global geography, seasonal insolation variations, and a 70-m mixed-layer ocean with heat capacity but no horizontal transport of heat.
7. S. Manabe and R. J. Stouffer, *Nature (London)* **282**, 491 (1979); *J. Geophys. Res.* **85**, 5529 (1980).
8. J. Hansen, A. Lacis, D. Rind, G. Russell, P. Stone, in preparation. Results of an initial CO_2 experiment with this model are summarized in (*6*).
9. National Academy of Sciences, *Understanding Climate Change* (Washington, D.C., 1975).
10. R. E. Newell and T. G. Dopplick, *J. Appl. Meteorol.* **18**, 822 (1979).
11. S. B. Idso, *Science* **207**, 1462 (1980); *ibid.* **210**, 7 (1980).
12. *J. Geophys. Res.* **82** (No. 28) (1977); *ibid.* **85** (No. A13) (1980).
13. S. Manabe and R. T. Wetherald, *J. Atmos. Sci.* **24**, 241 (1967).
14. A. Lacis, W. Wang, J. Hansen, *NASA Weather and Climate Science Review* (NASA Goddard Space Flight Center, Greenbelt, Md., 1979).
15. R. A. McClatchey *et al.*, *U.S. Air Force Cambridge Res. Lab. Tech. Rep. TR-73-0096* (1973).
16. R. E. Roberts, J. E. A. Selby, L. M. Biberman, *Appl. Opt.* **15**, 2085 (1976).
17. O. B. Toon and J. B. Pollack, *J. Appl. Meteorol.* **12**, 225 (1976).
18. R. D. Cess, *J. Quant. Spectrosc. Radiat. Transfer* **14**, 861 (1974).
19. W. C. Wang and P. H. Stone, *J. Atmos. Sci.* **37**, 545 (1980).
20. R. D. Cess, *ibid.* **35**, 1765 (1978).
21. G. Garrett, *Dyn. Atmos. Oceans* **3**, 239 (1979); P. Müller, *ibid.*, p. 267.
22. S. L. Thompson and S. H. Schneider, *J. Geophys. Res.* **84**, 2401 (1979).
23. M. I. Hoffert, A. J. Callegari, C. T. Hsieh, *ibid.* **85**, 6667 (1980).
24. H. Oeschger, U. Siegenthaler, U. Schotterer, A. Gugelmann, *Tellus* **27**, 168 (1975).
25. W. S. Broecker, *Science* **189**, 460 (1975).
26. J. Hansen, A. Lacis, P. Lee, W. Wang, *Ann. N.Y. Acad. Sci.* **338**, 575 (1980).
27. H. H. Lamb, *Philos. Trans. R. Soc. London Ser. A* **255**, 425 (1970).
28. S. H. Schneider and C. Mass, *Science* **190**, 741 (1975).
29. J. B. Pollack, O. B. Toon, C. Sagan, A. Summers, B. Baldwin, W. Van Camp, *J. Geophys. Res.* **81**, 1971 (1976).
30. A. Robock, *J. Atmos. Sci.* **35**, 1111 (1978); *Science* **206**, 1402 (1979).
31. W. Cobb, *J. Atmos. Sci.* **30**, 101 (1973); R. Roosen, R. Angione, C. Klemcke, *Bull. Am. Meteorol. Soc.* **54**, 307 (1979).
32. C. Sagan, O. B. Toon, J. B. Pollack, *Science* **206**, 1363 (1979).
33. S. Manabe and R. F. Strickler, *J. Atmos. Sci.* **21**, 361 (1964).
34. V. Ramanathan, *Science* **190**, 50 (1975).
35. B. G. Mendonca, *Geophys. Monit. Clim. Change* 7 (1979).
36. R. Weiss, *J. Geophys. Res.*, in press.
37. R. A. Rasmusson and M. A. K. Khalil, *Atmos. Environ.* **15**, 883 (1981).
38. F. S. Rowland and M. J. Molina, *Rev. Geophys. Space Phys.* **13**, 1 (1975).
39. R. L. Jenne, *Data Sets for Meteorologial Research* (NCAR-TN/IA-111, National Center for Atmospheric Research, Boulder, Colo., 1975); *Monthly Climate Data for the World* (National Oceanic and Atmospheric Administration, Asheville, N.C.).
40. T. P. Barnett, *Mon. Weather Rev.* **106**, 1353 (1978).
41. S. K. Kao and J. F. Sagendorf, *Tellus* **22**, 172 (1970).
42. R. A. Madden, *Mon. Weather Rev.* **105**, 9 (1977).
43. W. A. R. Brinkman, *Quart. Res. (N.Y.)* **6**, 335 (1976); I. I. Borzenkova, K. Ya. Vinnikov, L. P. Spirina, D. I. Stekhnovskiy, *Meteorol. Gidrol.* 7, 27 (1976); P. D. Jones and T. M. L. Wigley, *Clim. Monit.* **9**, 43 (1980).
44. P. E. Damon and S. M. Kunen, *Science* **193**, 447 (1976).
45. J. E. Hansen, W.-C. Wang, A. A. Lacis, *ibid.* **199**, 1065 (1978).
46. R. Oliver, *J. Appl. Meteorol.* **15**, 933 (1976); C. Mass and S. Schneider, *J. Atmos. Sci.* **34**, 1995 (1977).
47. J. M. Mitchell, in *Global Effects of Environmental Pollution*, S. F. Singer, Ed. (Reidel, Dordrecht, Netherlands, 1970), p. 139.
48. D. V. Hoyt, *Clim. Change* **2**, 79 (1979); *Nature (London)* **282**, 388 (1979).
49. K. Ya. Kondratyev and G. A. Nikolsky, *Q. J. R. Meteorol. Soc.* **96**, 509 (1970).
50. R. A. Madden and V. Ramanathan [*Science* **209**, 763 (1980)] make a similar comparison for the 60°N latitude belt. It is generally more difficult to extract the signal due to a global perturbation from a geographically limited area.
51. W. W. Kellogg and R. Schware, *Climate Change and Society* (Westview, Boulder, Colo., 1978).
52. CLIMAP Project Members, *Science* **191**, 1131 (1976).
53. H. H. Lamb, *Climate: Present, Past and Future* (Methuen, London, 1977), vol. 2.
54. W. W. Kellogg, in *Climate Change*, J. Gribbin, Ed. (Cambridge Univ. Press, Cambridge, 1977), p. 205; *Annu. Rev. Earth Planet. Sci.* **7**, 63 (1979).
55. J. J. Mercer, *Nature (London)* **271**, 321 (1978); T. Hughes, *Rev. Geophys. Space Phys.* **15**, 1 (1977).
56. C. L. Parkinson and W. W. Kellogg, *Clim. Change* **2**, 149 (1979).
57. R. C. Willson, S. Gulkis, M. Janssen, H. S. Hudson, G. A. Chapman, *Science* **211**, 700 (1981).
58. S. H. Schneider and S. L. Thompson, *J. Geophys. Res.*, in press.

59. We thank J. Charney, R. Dickinson, W. Donn, D. Hoyt, H. Landsberg, M. McElroy, L. Ornstein, P. Stone, N. Untersteiner, and R. Weiss for helpful comments; I. Shifrin for several typings of the manuscript; and L. DelValle for drafting the figures.